https://doi.org/10.1016/j.applthermaleng.2010.01.033

Lee, S.H., Yik, F.W.H., Lai, J.H.K. and Lee, W.L. (2010), Performance modelling of air cooled twin-circuit screw chiller, Applied Thermal Engineering, Vol. 30, No. 10, pp. 1179-1187

Performance modelling of air-cooled twin-circuit screw chiller

Lee SH[a], Yik FWH[a,*], Lai JHK[a] and Lee WL[a]

[a] Department of Building Services Engineering, The Hong Kong Polytechnic University, Hunghom, Kowloon, Hong Kong SAR, China

Abstract

Presented in the paper is a mathematical model for an air-cooled twin-circuit chiller, with two screw compressors per circuit. The chiller model comprises a series of linked mathematical modules, each made up of a set of thermodynamic and empirical equations for modelling the major components of the chiller. The coefficients in the component models were evaluated using rated operating conditions obtained from the manufacturer and recorded operation data of an existing chiller. The chiller model had been applied to simulate the performance of another set of chiller of the same make and model. Comparison of the predicted and recorded performance of the chiller showed that the model could yield accurate energy use predictions over a wide range of operating conditions. The model is also able to provide good predictions of the variation in chiller performance due to staged operation of the separate refrigerant circuits in the chiller and of compressors in each circuit, which match with observations made with measured chiller operation data.

Keywords: Air-cooled screw chiller; twin refrigerant circuits; multiple compressors; simulation model; verification of predictions.

(July 2009)

* Corresponding author. Tel.:+852 27665841
Email address: bewhyik@polyu.edu.hk (Yik FWH)

Performance modelling of air-cooled twin-circuit screw chiller

Nomenclatures

A	Nozzle throat area of each compressor [m^2]
AU_{A1}	Overall heat transfer coefficient of the evaporator at first section of circuit A of chiller [kW/^{o}C]
AU_{A2}	Overall heat transfer coefficient of the evaporator at last section of circuit A of chiller [kW/^{o}C]
AU_{cdA}	Overall heat transfer coefficient of the condenser at circuit A of chiller [kW/^{o}C]
AU_{cdB}	Overall heat transfer coefficient of the condenser at circuit B of chiller [kW/^{o}C]
AU_{evpA}	Overall heat transfer coefficient of the evaporator at circuit A of chiller [kW/^{o}C]
AU_{evpB}	Overall heat transfer coefficient of the evaporator at circuit B of chiller [kW/^{o}C]
c_a	Specific heat capacity of air [kJ/kg^{o}C]
c_{pv}	Specific heat capacity of vapour refrigerant at evaporator [kJ/kg^{o}C]
c_w	Specific heat capacity of water [kJ/kg^{o}C]
COP	Coefficient of performance of chiller
ε_{A1}	Evaporator effectiveness at first section of circuit A of chiller
ε_{A2}	Evaporator effectiveness at last section of circuit A of chiller
ε_{cdA}	Condenser effectiveness at circuit A of chiller
ε_{cdB}	Condenser effectiveness at circuit B of chiller
ε_{evpA}	Evaporator effectiveness at circuit A of chiller
ε_{evpB}	Evaporator effectiveness at circuit B of chiller
h_{A1}	Specific enthalpy of superheated refrigerant leaving evaporator at circuit A of chiller [kJ/kg]
$h_{A1,S}$	Specific enthalpy of saturated refrigerant leaving evaporator at circuit A of chiller [kJ/kg]
h_{A2}	Specific enthalpy at the compressor's discharge at circuit A of chiller [kJ/kg]
h_{A3}	Specific enthalpy at the condenser's discharge at circuit A of chiller [kJ/kg]

h_{A4} Specific enthalpy entering evaporator at circuit A of chiller [kJ/kg]

h_{B1} Specific enthalpy of superheated refrigerant leaving evaporator at circuit B of chiller [kJ/kg]

$h_{B1,S}$ Specific enthalpy of saturated refrigerant leaving evaporator at circuit B of chiller [kJ/kg]

h_{B2} Specific enthalpy at the compressor's discharge at circuit B of chiller [kJ/kg]

h_{B3} Specific enthalpy at the condenser's discharge at circuit B of chiller [kJ/kg]

h_{B4} Specific enthalpy entering evaporator at circuit B of chiller [kJ/kg]

m_w Mass flow rate of chilled water [kg/s]

m_{refA} Refrigerant flow rate at circuit A of chiller [kg/s]

m_{refB} Refrigerant flow rate at circuit B of chiller [kg/s]

η_{isen} Isentropic efficiency

η_{cc} Combined motor and transmission efficiency

N_A Number of operating condenser fans in circuit A

N_B Number of operating condenser fans in circuit B

N_{tot} Total number of staged condenser fans

PLR Chiller part load ratio

P_{cdA} Condensing pressure at circuit A of chiller [kPa]

P_{cdB} Condensing pressure at circuit B of chiller [kPa]

P_{evpA} Evaporating pressure at circuit A of chiller [^{o}C]

P_{evpB} Evaporating pressure at circuit B of chiller [^{o}C]

Q_A Cooling load at circuit A of chiller [kW]

Q_{A1} Cooling load at first section of circuit A of chiller [kW]

Q_{A2} Cooling load at last section of circuit A of chiller [kW]

Q_B Cooling load at circuit B of chiller [kW]

Q_{evp} Total cooling load of chiller [kW]

Q_{fl} Nominal cooling capacity of chiller [kW]

T_{cdA} Condensing temperature at circuit A of chiller [^{o}C]

T_{cdB} Condensing temperature at circuit B of chiller [°C]

T_{evpA} Evaporating temperature at circuit A of chiller [°C]

T_{evpB} Evaporating temperature at circuit B of chiller [°C]

ΔT_{evsh} Degree of superheat at the suction of the compressor [°C]

T_r Chilled water return temperature [°C]

T_s Chilled water supply temperature [°C]

T_{s1} Chilled water temperature entering circuit B's evaporator [°C]

T_{s2} Chilled water temperature leaving circuit B's evaporator [°C]

v_{A1} Specific volume of refrigerant at compressor suction of circuit A [m^3/kg]

$v_{A1,S}$ Specific volume of saturated vapour refrigerant at evaporator of circuit A [m^3/kg]

v_{B1} Specific volume of refrigerant at compressor suction of circuit B [m^3/kg]

$v_{B1,S}$ Specific volume of saturated vapour refrigerant at evaporator of circuit B [m^3/kg]

γ Mean isentropic coefficient

V_f Volumetric displacement rate of each compressor [m^3/s]

V_{pump1} Diverted refrigerant flow rate of each compressor at circuit A of chiller [m^3/s]

V_{pump2} Diverted refrigerant flow rate of each compressor at circuit B of chiller [m^3/s]

W_A Compressor power at circuit A of chiller [kW]

$W_{A,isen}$ Isentropic work input to compressor at circuit A of chiller [kJ/kg]

W_B Compressor power at circuit B of chiller [kW]

$W_{B,isen}$ Isentropic work input to compressor at circuit B of chiller [kJ/kg]

W_{Af} Fan power at circuit A of chiller [kW]

W_{Bf} Fan power at circuit B of chiller [kW]

1. Introduction

So far, vapour compression chillers are the most widely used type of chillers in central air-conditioning systems of modern buildings, but they are intensive energy consumers. For

instance, chillers alone may already account for up to 35–40% of the annual electricity consumption of an office building in Hong Kong [1]. Chiller performance modelling is a very useful technique to development of optimized chiller control strategies [2] and automatic detection and diagnosis of chiller and sensor faults [3], which can help optimize chiller energy use and avoid waste of energy due to chiller and sensor faults.

Various empirical, physical and dynamic modelling techniques have been employed to model the performance of chillers [4]. Empirical models are either 'black-box' or 'grey-box' models developed based on curve-fit or thermodynamic models established from empirical data. Such models [e.g. 5, 6] are relatively straightforward to establish but their application is limited to the specific chillers from which the empirical data were obtained. Physical models [e.g. 7] developed based on fundamental governing principles, such as mass and energy conservation, are more detailed and more widely applicable, but they are also more difficult to establish and use, as they usually involve a wide range of characteristic parameters of the modelled chiller which could be difficult to quantify. Dynamic modelling [e.g. 8] is similar to physical modelling, but takes into account the rate of change of the system variables with time.

Although a large variety of chiller models have been developed, few are for air-cooled screw chillers and among them, none can model in detail chillers that comprise multiple, separate refrigerant circuits, despite that this type of chillers is already widely used for its good part-load performance. Chan & Yu developed an air-cooled screw chiller model with four refrigeration circuits [9, 10] by assuming that the evaporators in the four refrigeration circuits would operate in parallel, as depicted in Figure 1. This implies that the same amount of heat transfer surface in the entire evaporator would remain available for cooling the chilled water

even if only one circuit was in operation [10]. In reality, however, the evaporator is compartmentalized with each compartment belonging to one refrigerant circuit.

<Figure 1>

Presented in this paper is a steady-state thermodynamic model for an air-cooled chiller with two separate refrigerant circuits, denoted as circuits A and B, and two screw compressors per circuit, as shown in Figure 2. The evaporator shell comprises two separate compartments, each connected to one refrigerant circuit. The tubes inside the evaporator are in a two-pass arrangement allowing chilled water to flow within the tubes from one shell compartment to the other and back. The evaporator model comprises three sections; the first and the third section jointly represent the shell compartment in circuit A and the second section represents the shell compartment in circuit B, which would allow the heat exchange between the chilled water and the refrigerant in the two circuits to be properly modelled.

<Figure 2>

In the next section, the characteristics of the chiller being modelled and the modelling assumptions made are described. The methods used to model the performance of individual chiller components are described in Section 3. Section 4 is on evaluation of the coefficients in the models, which was based on performance data records of an existing chiller. A comparison of the model predictions with measured operating data of another chiller of the same make and model is presented in Section 5.

2. Characteristics of the modelled chiller

Measured chiller performance data were collected from an existing chiller plant to provide a basis for the chiller model development work and for verification of the model predictions. There are five identical air-cooled twin-circuit screw chillers in the plant, each with a cooling

capacity of 300 tons of refrigeration (TR, 1TR = 3.517kW). For each refrigerant circuit, there are two identical screw compressors, one electronic expansion valve, and four heat rejection fans, and these components are identical between the two circuits. The refrigerant used is R134a. Other key characteristics of the chillers are summarized in Table 1.

<Table 1>

Since any one of the two circuits (circuits A & B, Figure 2), or both, in a chiller may be operated at any one time, and each circuit may have its cooling output adjusted independently from each other through varying the refrigerant flow rates in the two circuits, knowledge about the automatic control strategy being used to distribute the load between the two circuits and to sequence the operation of the compressors in each circuit is crucial to the development of a model for the chiller. However, this information was not given in the chiller manufacturer's catalogue while the local chiller supplier could not provide the information. Fortunately, the total power demands of the compressors in the two refrigerant circuits were separately measured and recorded by the building management system, which allowed the control strategy to be identified by observing the changes in the power demands.

Inspection of the available chiller power demand records unveiled that the operating sequence of the two refrigerant circuits in a chiller was as shown in Figure 3, which was based on the observations described below:

1. When the cooling load on the chiller was small but rising, only one circuit would be operated until the circuit was loaded to slightly exceeding half of the total cooling capacity of the chiller at which time the other circuit would be called upon to operate.

2. When the two circuits were operating simultaneously, the compressor power demands of the two circuits were approximately equal.

3. When both circuits operated together and the load dropped to about 40% of the total cooling capacity of the chiller, the circuit that came into operation earlier would be shut down.

<Figure 3>

Based on these observations, the sequencing control strategy assumed in the model is that circuit A will be started first when the part-load ratio (*PLR*) of the chiller is lower than 0.52. Both circuits will be run whenever the *PLR* exceeds 0.52. Circuit A will be stopped when the *PLR* drops to 0.42. When the load rises again, both circuits will be run when the *PLR* goes beyond 0.52. This time, when the *PLR* falls to 0.42, circuit B will be stopped. The cycle will be repeated until the chiller is shut-down. The method for determining the number of compressors to be run in each circuit is described in the next section together with descriptions on the compressor model.

Furthermore, since the two circuits comprise identical components and the total power demands of compressors in the two circuits, when both are in operation, were found to be approximately equal, it is considered reasonable to assume that the two circuits have equal rated cooling capacity and would each output half of the total cooling output when both circuits are in operation.

Since details about the head pressure control algorithm used in the chiller to cycle on and off the condenser fans were also unknown, the assumption was made that the condenser fans would be cycled on and off with reference to a high and a low condensing temperature settings. When the condensing temperature of the refrigerant in the condenser exceeds the high setting, more condenser fans would be switched on one by one until the condensing temperature drops below the high setting or all fans are running. The number of running condenser fans will remain unchanged as long as the condensing temperature stays within the

dead-band between the high and the low settings. When the condensing temperature drops below the low setting, the running condenser fans will be switched off one by one until the condensing temperature rises above the low setting or all fans are stopped. The high and low settings were determined by observing the records of condensing temperatures (Figure 4), and were taken as 55°C and 42°C respectively.

<Figure 4>

In addition to the abovementioned assumptions, development of the chiller model was based on the following assumptions:

1. The simplified vapour compression cycle shown in Figure 5 applies to both circuits;
2. The expansion valve will keep the state of the refrigerant entering the compressor at a degree of superheat of 3ºC at all times [10];
3. The refrigerant pressure drops across the condenser and the evaporator are negligible;
4. The refrigerant enthalpy will remain unchanged as it passes through the expansion device;
5. The refrigerant leaving the condenser is at a saturated liquid state without sub-cooling; and
6. Heat exchange between the refrigeration system and its surroundings is negligible.

The last assumption implies that the heat rejection rate at the condenser will always be equal to the sum of the cooling output rate at the evaporator and the power input to the compressors.

<Figure 5>

3. Model development

Given that the chiller has two refrigeration circuits, circuits A and B, the chiller may operate in any one of the following three modes:

a. Only circuit A operates

b. Only circuit B operates

c. Both circuits operate

Since the same model can be used to simulate either circuit in the chiller while only one of the two circuits is in operation, a model for a single circuit (circuit A) and a model for both circuits in operation were developed, as described below.

3.1. Evaporator of circuit A

When only circuit A operates, the cooling output of the evaporator can be related to the properties of the chilled water and the refrigerant, as shown in equations (1) to (3).

$$Q_A = m_w \cdot c_w \cdot (T_r - T_s) \quad (1)$$

$$Q_A = m_{refA} \cdot (h_{A1} - h_{A3}) \quad (2)$$

$$Q_A = \varepsilon_{evpA} \cdot m_w \cdot c_w \cdot (T_r - T_{evpA}) \quad (3)$$

Where ε_{evpA}, the evaporator effectiveness, in equation (3) is given by:

$$\varepsilon_{evpA} = 1 - \exp(-\frac{AU_{evpA}}{m_w \cdot c_w}) \quad (4)$$

The term AU_{evpA} in equation (4), the overall heat transfer coefficient of the evaporator, can be expressed as a function of the chilled water flow rate and the cooling output rate as shown in equation (5) [11]. The coefficients a_1, a_2 and a_3 in the model have to be evaluated based on operating data of the specific chiller to be modelled (see Section 4).

$$AU_{evpA} = \frac{1}{a_1 \cdot m_w^{-0.8} + a_2 \cdot Q_A^{-0.745} + a_3} \tag{5}$$

Equations (1) & (3) can be combined to yield the following equation for evaluation of the evaporating temperature of the refrigerant.

$$T_{evpA} = T_s + \frac{Q_A}{m_w \cdot c_w}\left(1 - \frac{1}{\varepsilon_{evpA}}\right) \tag{6}$$

Having evaluated T_{evpA}, the corresponding refrigerant evaporating pressure can be determined using the Clausius-Clapeyron equation below [12].

$$P_{evpA} = \exp\left(a + \frac{b}{T_{evpA} + 273.15}\right) \tag{7}$$

The values of the coefficients in the above equation are: a = 15.489 and b = –2681.99.

3.2. Compressors in circuit A

The actual power input to the staged compressors in circuit A is given by [12]:

$$W_A = m_{refA} \cdot \frac{w_{A,isen}}{\eta_{isen} \cdot \eta_{cc}} \tag{8}$$

Where, from equation (2), m_{refA}, the refrigerant mass flow rate, is given by:

$$m_{refA} = \frac{Q_A}{h_{A1} - h_{A3}} \tag{9}$$

The isentropic compressor work per unit mass of refrigerant is given by [9]:

$$w_{A,isen} = \frac{\gamma}{\gamma - 1} \cdot P_{evpA} \cdot v_{A1} \cdot \left[\left(\frac{P_{cdA}}{P_{evpA}} \right)^{\frac{\gamma-1}{\gamma}} - 1 \right] \tag{10}$$

The constant coefficient γ for the refrigerant R134a is 1.072 [12]. The specific volume of the superheated refrigerant at the compressor suction (v_{A1}) in equation (10) can be evaluated from the saturated specific volume of the refrigerant in the evaporator, $v_{A1,s}$, the refrigerant degree of superheat at the compressor suction, ΔT_{evsh}, and the evaporating pressure of the refrigerant in the evaporator, P_{evpA}, using equation (11) [8].

$$\frac{1}{v_{A1}} = \frac{1}{v_{A1,s}} - (-0.0007 + 0.00002 \cdot P_{evpA}) \cdot \Delta T_{evsh} \tag{11}$$

The following regression model for screw compressor developed by Solati [13] was used in the chiller model for evaluating the isentropic efficiency (η_{isen}):

$$\begin{aligned} \eta_{isen} = 0.01 \cdot (& a_1 \cdot T_{cdA}{}^2 + a_2 \cdot T_{cdA} + a_3 \cdot T_{evpA}{}^2 + a_4 \cdot T_{evpA} \\ & + a_5 \cdot T_{cdA}{}^2 \cdot T_{evpA} + a_6 \cdot T_{cdA} \cdot T_{evpA} + a_7 \cdot Q_{fl} + a_8) \end{aligned} \tag{12}$$

Where

$a_1 = -0.0316958$ $a_2 = 2.90112$ $a_3 = -0.0296849$ $a_4 = -1.45279$

$a_5 = 0.000321176$ $a_6 = 0.00683086$ $a_7 = 0.00170575$ $a_8 = -16.5018$

The combined motor and transmission efficiency (η_{cc}) for a single compressor and two compressors working in parallel can be determined using equations (13) & (14) but the coefficients b_1 to b_3 and c_1 to c_3 had to be estimated by regression using operating data of the chiller (see Section 4):

$$\eta_{cc} = b_1 + b_2 \cdot PLR + b_3 \cdot PLR^2 \text{, for a single compressor in operation} \quad (13)$$

$$\eta_{cc} = c_1 + c_2 \cdot PLR + c_3 \cdot PLR^2 \text{, for two compressors in operation} \quad (14)$$

The refrigerant flow rate (m_{refA}) through a single compressor can also be determined using equation (15) for the full load condition and equation (16) for the part load condition [12]. Equation (16) differs from equation (15) only in the additional term V_{pumpA}, which is the refrigerant flow rate that is re-circulated to suction when the sliding valve is opened under part-load operation [12].

$$m_{refA} = \frac{1}{v_A} \cdot \left[V_f - A \cdot \sqrt{P_{evpA} \cdot v_A} \cdot \left(\frac{P_{cdA}}{P_{evpA}}\right)^{\frac{\gamma+1}{2\cdot\gamma}} \cdot \sqrt{\gamma \left(\frac{2}{\gamma+1}\right)^{\frac{\gamma+1}{\gamma-1}}} \right] \quad (15)$$

$$m_{refA} = \frac{1}{v_A} \cdot \left[V_f - V_{pumpA} - A \cdot \sqrt{P_{evpA} \cdot v_A} \cdot \left(\frac{P_{cdA}}{P_{evpA}}\right)^{\frac{\gamma+1}{2\cdot\gamma}} \cdot \sqrt{\gamma \left(\frac{2}{\gamma+1}\right)^{\frac{\gamma+1}{\gamma-1}}} \right] \quad (16)$$

If the refrigerant flow rate determined using equation (9) exceeds the refrigerant flow rate determined using equation (15), which corresponds to the condition where one compressor is running at full load condition, then both compressors in the circuit would need to be run to cope with the load. However, if the reverse is true, then V_{pumpA} will have to be equal to or greater than zero in order that the refrigerant flow rates estimated from equations (9) & (16) will agree with each other, which means that only one compressor needs to be run under that condition. This is how the number of compressor(s) in a circuit to be run is determined in the chiller model. The volumetric displacement (V_f) and the nozzle area (A) of each compressor had to be estimated based on the manufacturer's performance data for the full-load condition (see Section 4).

The specific enthalpy of the superheated refrigerant at the discharge and suction sides of the compressor (h_{A2} & h_{A1}) can be found using equations (17) & (18).

$$h_{A2} = h_{A1} + \frac{w_{A,isen}}{\eta_{isen} \cdot \eta_{cc}} \tag{17}$$

$$h_{A1} = h_{A1,s} + c_{pv} \cdot \Delta T_{evsh} \tag{18}$$

3.3. Condenser in circuit A

The heat rejection rate in the condenser in circuit A can be described by the following equations:

$$Q_{cdA} = Q_A + W_A \tag{19}$$

$$Q_{cdA} = m_a \cdot c_a \cdot (T_{ao} - T_{out}) \tag{20}$$

$$Q_{cdA} = m_{refA} \cdot (h_{A2} - h_{A3}) \tag{21}$$

$$Q_{cdA} = \varepsilon_{cdA} \cdot m_a \cdot c_a \cdot (T_{cdA} - T_{out}) \tag{22}$$

Where

$$\varepsilon_{cdA} = 1 - \exp(-\frac{AU_{cdA}}{m_a \cdot c_a}) \tag{23}$$

$$AU_{cdA} = d_1 \cdot Q_{cdA}^{\ d2} m_a^{\ d3} \tag{24}$$

Equation (19) is based on the assumption that the refrigeration system is isolated from the surroundings. Equations (20) & (21) relate the heat rejection rate to the states and flow rates of the condenser air and refrigerant while equation (22) relates the heat rejection rate to the

condensing temperature of the refrigerant (T_{cdA}) and the leaving air temperature (T_{out}), using the effectiveness method, with the heat transfer effectiveness (ε_{cdA}) described in equation (23). For the overall heat transfer coefficient AU_{cdA} of the condenser shown in equation (24), the coefficients d_1 to d_3 were estimated by regression based on available chiller performance data (see Section 4). The condensing temperature and the condensing pressure can finally be estimated using equations (25) & (26) respectively.

$$T_{cdA} = T_{out} + \frac{Q_{cdA}}{\varepsilon_{cdA} \cdot m_a \cdot c_a} \tag{25}$$

$$P_{cdA} = \exp(a + \frac{b}{T_{cdA} + 273.15}) \tag{26}$$

Values of the coefficients a & b in equation (26) are same as those in equation (7) mentioned above.

The condenser air mass flow rate, m_a, in the above condenser model would vary depending on the number of condenser fan(s) being run under the head pressure control of the chiller. As discussed in Section 2, cycling on and off of condenser fans is determined by comparing the refrigerant condensing temperature with the high and low temperature settings. In each new time-step, the number of condenser fan(s) that should be run, N_A, will first be assumed to be equal to that in the previous time step (when the chiller has just been started, this number will be set at 1), but whether this number of condenser fan(s) would be sufficient to keep the condensing temperature within the dead-band between the high and low settings will be checked. If the condensing temperature is found to be over 55°C or below 42°C, the number of fan(s) to be run will be adjusted up or down by one at a time, and the condensing temperature of the refrigerant will be checked again each time until the condensing temperature is kept within the dead-band or all or no fans are running.

Having determined the number of fan(s) to be run, m_a can be determined, as follows:

$$m_a = \frac{N_A}{N_{tot}} \cdot m_{a,tot} \tag{27}$$

3.4. *Expansion valve in Circuit A*

The modelled chiller is equipped with an electronic expansion valve. Inside the expansion valve, a piston is driven by an electronically controlled linear stepper motor to move up and down to vary the cross sectional area of the refrigerant flow path such that the refrigerant is kept in a superheated vapour state at the suction side of the compressor. A series of calibrated orifices are installed into the wall of the refrigerant inlet port. When the refrigerant passes through the orifices, the refrigerant expands and becomes a mixture of liquid and gas. Despite the complex components involved, in the chiller model, the expansion device is modelled simply by assuming that the throttling process is adiabatic, thus the entering and leaving enthalpies of the refrigerant are equal, as depicted by equation (28).

$$h_{A3} = h_{A4} \tag{28}$$

3.5. *COP of circuit A*

The *COP* of circuit A of the chiller, when only circuit A is in operation (same applies when only circuit B is in operation), as defined in equation (29), takes into account the cooling output (Q_A), the total compressor power (W_A) and the condenser fan power (W_{Af}).

$$COP_A = \frac{Q_A}{W_A + W_{Af}} \tag{29}$$

3.6. Chiller model when both circuits A & B are in operation

The evaporator of a twin-circuit chiller is modelled by breaking it down into three heat exchangers in series, as shown in Figure 6.

<Figure 6>

The two heat exchangers at both ends represent the evaporator in circuit A and that in the middle represents the evaporator in circuit B, which mimic the path through which the chilled water will flow through the two shell compartments of the evaporator. The water tubes in the two heat exchangers at the two ends are submerged in the same bath of evaporating refrigerant at the shell side of the part of the evaporator in circuit A, and thus the evaporating temperature and pressure of the refrigerant in these two heat exchangers are identical. The cooling output of circuit A, Q_A, is the sum of cooling output of the first and the last heat exchangers, i.e.:

$$Q_A = Q_{A1} + Q_{A2} \tag{30}$$

It follows that:

$$Q_{A1} = m_w \cdot c_w \cdot (T_r - T_{s1}) \tag{31}$$

$$Q_B = m_w \cdot c_w \cdot (T_{s1} - T_{s2}) \tag{32}$$

$$Q_{A2} = m_w \cdot c_w \cdot (T_{s2} - T_s) \tag{33}$$

By assuming that Q_B equals half of the total cooling output of the chiller, the value of (T_{s1} − T_{s2}) is known:

$$(T_{s1} - T_{s2}) = \frac{Q_B}{m_w c_w} \tag{34}$$

The heat transfers from the chilled water to the evaporating refrigerant in the evaporators are governed by the effectiveness equations shown below:

$$Q_{A1} = \varepsilon_{A1} \cdot m_w \cdot c_w \cdot (T_r - T_{evpA}) \tag{35}$$

$$Q_{A2} = \varepsilon_{A2} \cdot m_w \cdot c_w \cdot (T_{s2} - T_{evpA}) \tag{36}$$

$$Q_B = \varepsilon_{evpB} \cdot m_w \cdot c_w \cdot (T_{s1} - T_{evpB}) \tag{37}$$

The effectiveness of the three heat exchangers and the overall heat transfer coefficient for the part of the evaporator in circuit B are as shown in equations (38) to (41) below.

$$\varepsilon_{A1} = 1 - \exp(-\frac{AU_{A1}}{m_w \cdot c_w}) \tag{38}$$

$$\varepsilon_{A2} = 1 - \exp(-\frac{AU_{A2}}{m_w \cdot c_w}) \tag{39}$$

$$\varepsilon_{evpB} = 1 - \exp(-\frac{AU_{evpB}}{m_w \cdot c_w}) \tag{40}$$

$$AU_{evpB} = \frac{1}{a_1 \cdot m_w^{-0.8} + a_2 \cdot Q_B^{-0.745} + a_3} \tag{41}$$

In the model, the assumption is made that the overall heat transfer coefficients AU_{A1} and AU_{A2} are approximately equal, as depicted by equation (42), and that equation (5) for the overall heat transfer heat coefficient of the part of the evaporator in circuit A (AU_{evpA}) remains valid.

$$AU_{A1} \cong AU_{A2} \cong 0.5 \cdot AU_{evpA} \tag{42}$$

Based on the above equations, the following iterative steps are used to estimate T_{evpB}.

1. Assume a value for T_{evpA}.

2. Using equation (35) and the assumed value of T_{evpA}, evaluate Q_{A1}.

3. Using this value of Q_{A1} and equation (31), evaluate T_{s1}.

4. Based on the assumption that $Q_A = Q_B = 0.5\ Q_{evp}$ and using this value of T_{s1} and equation (32), evaluate T_{s2} and then $Q_{A2} = Q_A - Q_{A1}$.

5. Using equation (36), T_{evpA} can be determined and checked with the value assumed in step 1. If the difference between them is large, the process will be repeated from step 1, taking the T_{evpA} value just estimated as the assumed value.

6. When a converged solution is found, T_{evpB} can be determined using equation (37).

For the other components, including the compressors, condensers and expansion valves, the same set of models developed for circuit A can be used for modelling the corresponding components in the two circuits when both are in operation.

3.7 The whole chiller model

A chiller simulation program has been developed by assembling the component models presented above. The inputs to the program include the chilled water supply (T_s) and return (T_r) temperatures and the outdoor air temperature (T_{out}) under the actual operating conditions. Since the chiller model includes component models the coefficients of which need to be determined based on operating data of the specific chiller to be modelled (see Section 4), it cannot be applied to simulate another chiller of a different make and model unless the component model coefficients have been re-established.

For each set of inputs corresponding to a particular operating condition, the model will first determine the cooling load on the chiller (Q_{evp}), based on the known (constant) chilled water flow rate (m_w) and the input chilled water supply and return temperatures (T_s & T_r), and then the part load ratio (*PLR*). With reference to the *PLR*, whether only one circuit or both circuits will have to be run can be decided. When only one circuit needs to be run, the abovementioned alternate sequencing algorithm will be used to decide whether circuit A or circuit B will be operated. The iterative procedure for determining the evaporating temperatures in circuit A and circuit B will be implemented only if both circuit needs to be run.

Because determination of the refrigerant mass flow rate, the compressor power and the heat rejection rate requires knowledge about the condensing temperature in the circuit (T_{cdA} &/or T_{cdB}) but the condensing temperature, in turn, can only be determined when the heat rejection rate is known, an iterative loop is implemented in the model to solve for the condensing temperature and the heat rejection rate simultaneously. Within this loop, there is another iterative loop for determination of the number of condenser fans that need to be run. These nested iterative loops are implemented for each operating circuit. The convergence criteria used in computing the evaporating and condensing temperatures are both 0.01°C.

When a converged solution has been obtained, the compressor and condenser fan power demand and the evaporating and condensing temperatures of each circuit, and the total chiller power demand and *COP* will be output. The program will then proceed to the next set of input until all cases have been processed.

4. Coefficient evaluation

As noted in the above descriptions on the chiller model, there are a series of model coefficients that need to be evaluated based on known performance data for the chiller being

modelled. For this purpose, the operating data of an existing chiller for a period of 4 months (from February to May) were retrieved from the building management system.

The unknown coefficients in equations (5) & (41) for the overall heat transfer coefficients of the evaporators AU_{evpA} & AU_{evpB} were evaluated using the available chiller operation data that were pertaining to the condition where only a single circuit was operating. First, equation (5) was re-organized into:

$$\frac{1}{AU_{evpA}} = a_1 \cdot m_w^{-0.8} + a_2 \cdot Q_A^{-0.745} + a_3 \tag{43}$$

For each operating condition, the value of AU_{evpA} was determined beforehand using equation (44) and the corresponding data available in the records. Based on equation (43), multiple linear regression method was then used to evaluate the coefficients a_1 to a_3. The values so evaluated for these coefficients were 0.1748, 0.0549 and 0 respectively (R^2 = 0.98), and they apply to the evaporator models of both circuits.

$$AU_{evp} = m_w \cdot c_w \cdot \ln\left(\frac{T_r - T_{evp}}{T_s - T_{evp}}\right) \tag{44}$$

The overall heat transfer coefficients of the condensers (AU_{cdA}, AU_{cdB}) are described by equation (24), which was re-organized into:

$$\ln(AU_{cdA}) = \ln(d_1) + d_2 \cdot \ln(Q_{cdA}) + d_3 \cdot \ln(m_a) \tag{45}$$

For each operation record, the condenser air flow rate (m_a) was determined from the rated flow rate of each fan and the number of operating fans. The latter was estimated from the ratio of the power consumed by the operating fans to the total rated fan power of the chiller. By adding the compressor power and the cooling output of the chiller, the heat rejection rate

(Q_{cdA}) was determined, which also allowed the leaving condenser air temperature (T_{out}) to be found by using equation (20) and, in turn, the value of AU_{cdA} to be found using equation (46). On the basis of equation (45) and the set of pre-calculated values for $\ln(AU_{cdA})$, $\ln(Q_{cdA})$ and $\ln(m_a)$, the coefficients $\ln(d_1)$, d_2 & d_3 were evaluated using multiple linear regression method. The values of d_1 to d_3 so evaluated were 1, 0.6429 and 0.015 respectively ($R^2 = 0.9$).

$$AU_{cd} = m_a \cdot c_a \cdot \ln\left(\frac{T_{cd} - T_{out}}{T_{cd} - T_{ao}}\right) \tag{46}$$

For the combined motor and transmission efficiency, it was also estimated using the chiller performance data for the condition where only one single circuit was in operation. By re-arranging equation (8):

$$\eta_{cc} = m_{refA} \cdot \frac{w_{A,isen}}{\eta_{isen} \cdot W_A} \quad ; \quad \text{when circuit A is in operation} \tag{47}$$

$$\eta_{cc} = m_{refB} \cdot \frac{w_{B,isen}}{\eta_{isen} \cdot W_B} \quad ; \quad \text{when circuit B is in operation}$$

The refrigerant flow rate (m_{refA} or m_{refB}), the isentropic power ($w_{A,isen}$ or $w_{B,isen}$) and the isentropic efficiency (η_{isen}) in equation (47) can be determined using equations (9), (10) & (12) respectively in conjunction with the available chiller performance data, which allowed a set of values for the combined motor and transmission efficiency (η_{cc}) corresponding to various operating conditions embraced by the available chiller performance data to be calculated. The unknown coefficients b_1 to b_3 in equation (13) for η_{cc} were then evaluated through multiple linear regression and the values found are -0.39, 1.4875 and 0.3043 respectively ($R^2 = 0.98$). Through a similar method, the values evaluated for the coefficients

c_1 to c_3 in equation (14) for η_{cc} for two compressors working in parallel were -0.3422, 1.5444 and -0.1707 respectively ($R^2 = 0.96$).

As to the volumetric displacement (V_f) and the nozzle area (A) of each compressor in equations (15) & (16), they were estimated based on the rated operating condition of the chiller as stated in the chiller manufacturer's catalogue. The volumetric displacement of each compressor was estimated using equation (48) [12] in which the power (W_A) is the rated power of one compressor of the chiller.

$$V_f = \frac{W_A \cdot (\gamma - 1)}{\gamma \cdot P_{evpA} \cdot \left[\left(\frac{P_{cdA}}{P_{evpA}} \right)^{\frac{\gamma-1}{\gamma}} - 1 \right]} \tag{48}$$

The nozzle throat area (A) of the compressor was calculated by re-arranging equation (15) into equation (49), with the refrigerant flow rate (m_{refA}) estimated using equation (9).

$$A = \frac{V_f - m_{refA} \cdot v_{A1}}{\sqrt{P_{evpA} \cdot v_{A1}} \cdot \left(\frac{P_{cdA}}{P_{evpA}} \right)^{\frac{\gamma+1}{2 \cdot \gamma}} \cdot \sqrt{\gamma \left(\frac{2}{\gamma+1} \right)^{\frac{\gamma+1}{\gamma-1}}}} \tag{49}$$

The results obtained were as follows:

Volumetric displacement of each compressor (V_f) = 0.5638m^3/s

Nozzle area of each compressor (A) = 0.00092m^2

5. Comparison of model predictions with chiller operating records

Besides the set of data used in evaluation of the model coefficients, another set of measured operating performance data for another chiller of the same make and model in the same plant for a period of 3 months (from August to October) was collected for a comparison with the

predictions of the chiller model. These data cover a wide range of part load ratio (*PLR*: 0.05-1.2) and outdoor air temperature (T_{out}: 22-37°C). Figures 7 to 11 show the comparisons of the model predictions with the recorded chiller operating data.

<Figures 7 to 11>

As shown in Figure 7, the predicted *COP* of the chiller agrees remarkably well with the *COP* calculated from the chiller load and power demand data, with about 96% of the predicted values falling within ±10% of the calculated values. The predicted evaporating temperatures in circuits A & B (T_{evpA} & T_{evpB}) of the chiller (Figures 8 & 9) also compare well with the measured data, with about 84% and 85% of the predictions falling within ±10% of the respective measured values. The data of each circuit shown in the corresponding figure include the operating conditions when the circuit was the only circuit being run and when the circuit was operating concurrently with the other circuit.

Although about 90% of the predictions were within ±10% of the measured values, the predicted condensing temperatures in circuits A and B (Figures 10 & 11) scatter about the measured values in several cluster bands. Nonetheless, such discrepancies should be an expected outcome because the accuracy of prediction of the condensing temperature is dependent on how accurately the number of condenser fans being run was predicted and any departure from the actual number would cause significant deviations between the predicted and the measured condensing temperature. With the wide dead-band used in determining whether or not to switch on or off condenser fans, having one more or one less fan running may not cause the condensing temperature to go above or below the high or low settings but the corresponding condensing temperatures could depart substantially from each other.

Comparison of the predicted number of circuit(s) being run with the measured records (indicated by the power demand of individual circuits) unveiled that only in less than 5% of the cases that the prediction deviated from the actual situation. When the control algorithm in the chiller model was disabled and replaced by the actual number of circuits in operation as ascertained from the measured records, the difference in the predicted energy use was found to be about 1% only.

Since the key improvement in chiller modelling method represented by the present chiller model is in its ability to model changes in chiller performance due to staged operation of the separate refrigerant circuits and of the compressors within each circuit, the predicted variation in *COP* with *PLR* was compared with the measured data. Figure 12 shows the total chiller *COP* predicted by the model for a range of *PLR* under the outdoor temperature of 28°C. This clearly shows that the chiller *COP* can rise and drop substantially as an additional compressor or refrigerant circuit is called upon to operate to cope with a rising load. Such a trend can also be observed from the measured data as shown in Figure 13.

<Figures 12 & 13>

7. Conclusion

In this paper, the model developed for an air-cooled twin-circuit screw chiller is presented and the chiller energy use predictions of the model have been verified to be in good agreement with measured data over a wide range of operating conditions. For chiller *COP*, 96% of the predictions fell within ±10% of the calculated values. The model is also able to provide good predictions of the variation in chiller performance due to staged operation of the separate refrigerant circuits in the chiller and of compressors in each circuit, which match with observations made with measured chiller operation data.

Acknowledgement

The authors thank the Hong Kong Polytechnic University for the funding support for the reported work. Thanks are also due to the Facility Management Office of the University for providing access to the chiller performance data.

References

[1] Chan KT, Yu FW. Part load efficiency of air cooled multiple chiller plant. Building Services Engineering Research and Technology 2002; 23 (1): 31-41.

[2] Chan KT, Yu FW. Optimum Setpoint of Condensing Temperature for Air-Cooled Chillers. HVAC&R Research 2004; 10: 113-127.

[3] Cui J, Wang SW. A model-based online fault detection and diagnosis strategy for centrifugal chiller systems, International Journal of Thermal Sciences 2005; 44(10): 986-999.

[4] Browne MW, Bansal PK. Different modelling strategies for in-situ liquid chillers. Proceedings of the Institute of Mechanical Engineers Part A: J. Power and Energy 2001; 215: 357-374.

[5] Leverenz DJ, Bergan NE. Development and validation of a reciprocating chiller model for hourly energy analysis programs. ASHRAE Transactions 1983; 89(1a): 156-174.

[6] Peitsman H, Bakker V. Application of black-box models to HVAC systems for fault detection. ASHRAE Transactions 1996; 102(1): 628-640.

[7] Browne MW, Bansal PK. Steady-state model of centrifugal liquid chillers. International Journal of Refrigeration 1998; 21(5): 343-358.

[8] Jia, Y. Model-Based Generic Approaches for Automated Fault Detection, Diagnosis, Evaluation (FDDE) and for Accurate Control of Field-Operated Centrifugal Chillers; PhD Thesis, Faculty of Drexel University; 2002.

[9] Chan KT, Yu FW. Thermodynamic-behaviour model for air-cooled screw chillers with a variable set-point condensing temperature. Applied Energy 2006; 83: 265-279.

[10] Yu FW, Chan KT. Tune up of the set point of condensing temperature for more energy efficient air cooled chillers. Energy Conversion and Management 2006; 47: 2499-2514.

[11] Wang SW, Wang J, Burnett J. Mechanistic model of centrifugal chillers for HVAC system dynamics simulation. Building Services Engineering Research & Technology 2000; 21(2): 73-83.

[12] Bourdouxhe JP, Grodent M, Lebrun JJ. HVAC1 Toolkit: Algorithms and Subroutines for Primary HVAC System Energy Calculations. The American Society of Heating, Refrigerating and Air Conditioning Engineers; 1997.

[13] Solati B. Computer modelling of the energy performance of screw chiller. MSc thesis, Department of Building, Civil and Environmental Engineering, Concordia University. Montreal, Quebec: Concordia University Press; 2002.

List of Table

List of Figures

Lee, S.H., Yik, F.W.H., Lai, J.H.K. and Lee, W.L. (2010), Performance modelling of air cooled twin-circuit screw chiller, Applied Thermal Engineering, Vol. 30, No. 10, pp. 1179-1187

Table 1 Characteristics of the chiller being modelled

Chiller characteristics	Value
Rated cooling capacity	1055kW
Rated chilled water entering / leaving temperatures	12˚C/7˚C
Rated chilled water flow rate	50*l*/s
Rated condenser air entering temperature	35˚C
Rated condenser air flow rate	42.77*l*/s
No. of condenser fans	8
Total condenser fan power	8kW
No. of compressors	4
Total rated compressor power	398kW

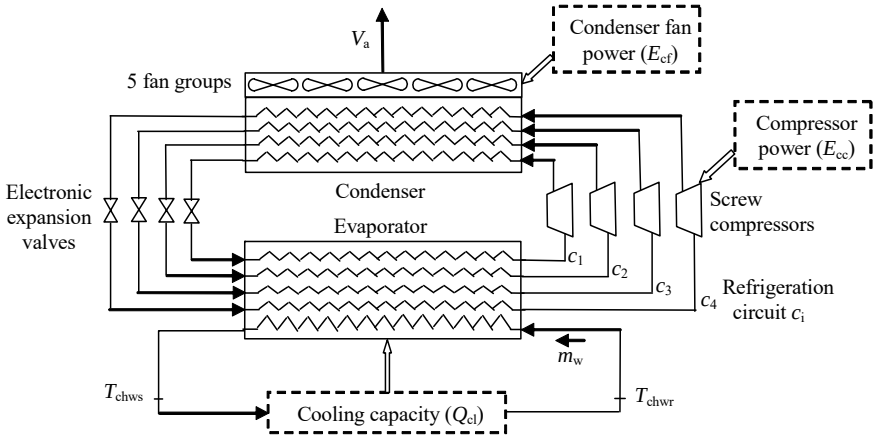

Figure 1 Systematic diagram of the chiller with four refrigeration circuits

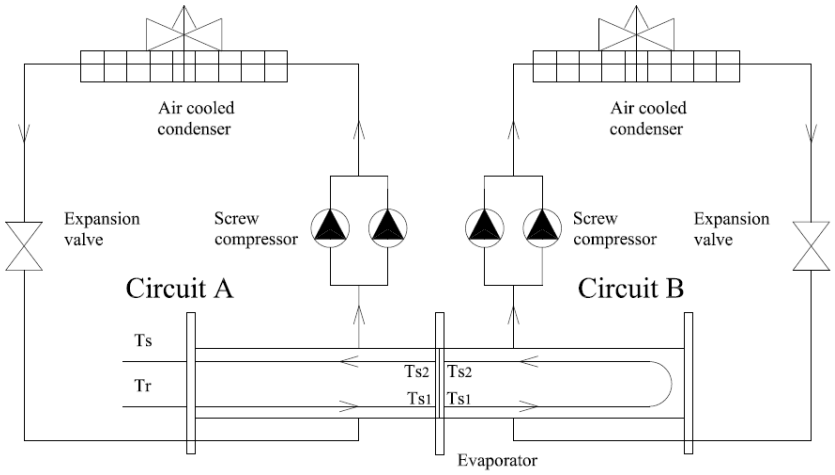

Figure 2 Schematic diagram for an air-cooled twin-circuit screw chiller

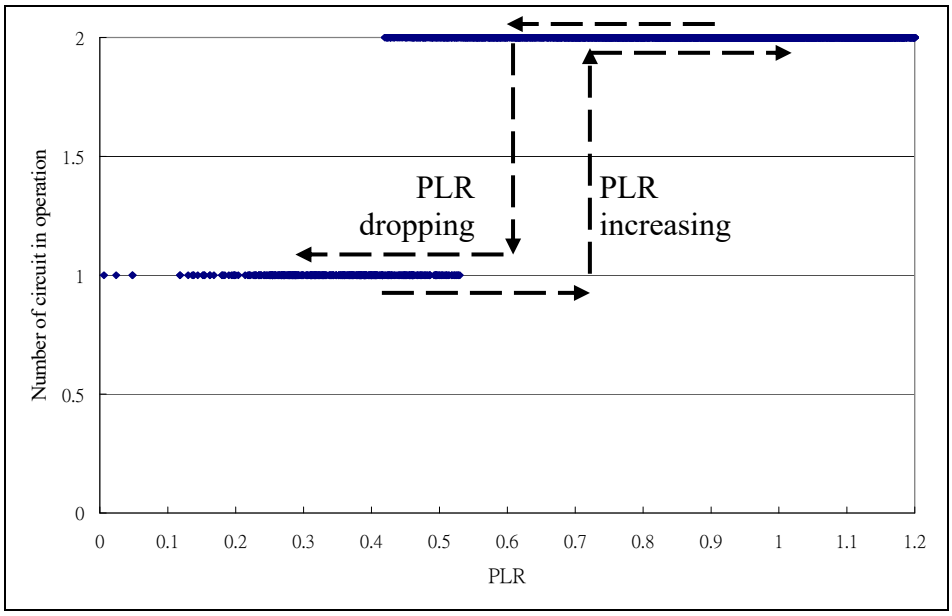

Figure 3 Number of refrigeration circuits in operation under rising and reducing cooling load on the chiller

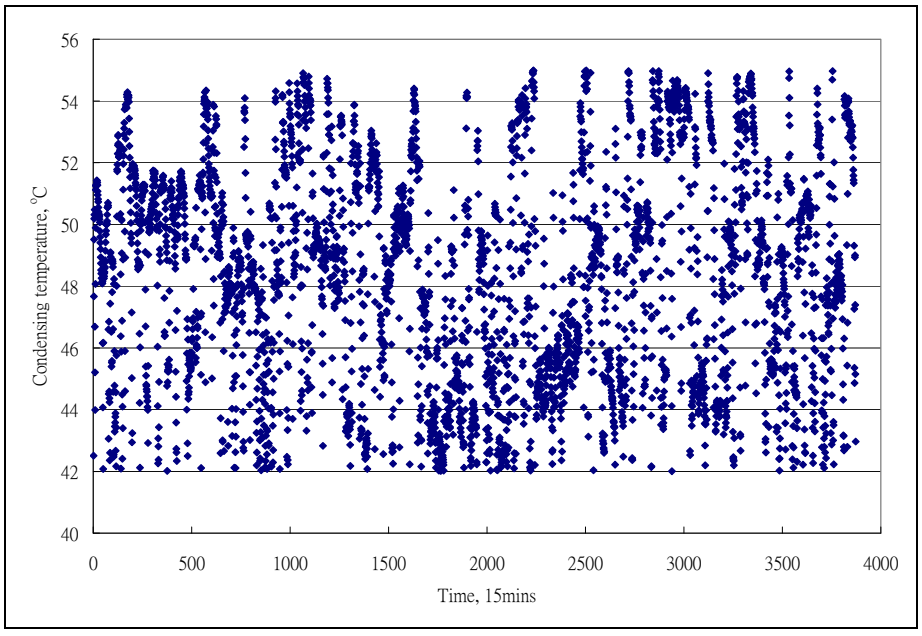

Figure 4 Condensing temperature records

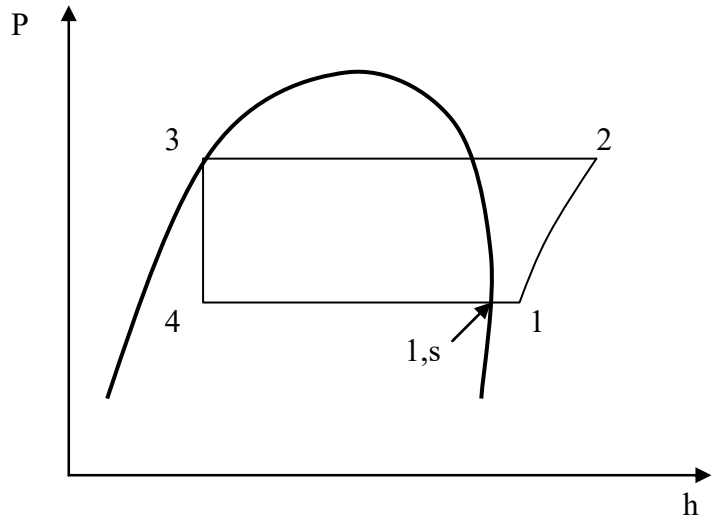

Figure 5 The assumed refrigeration cycle

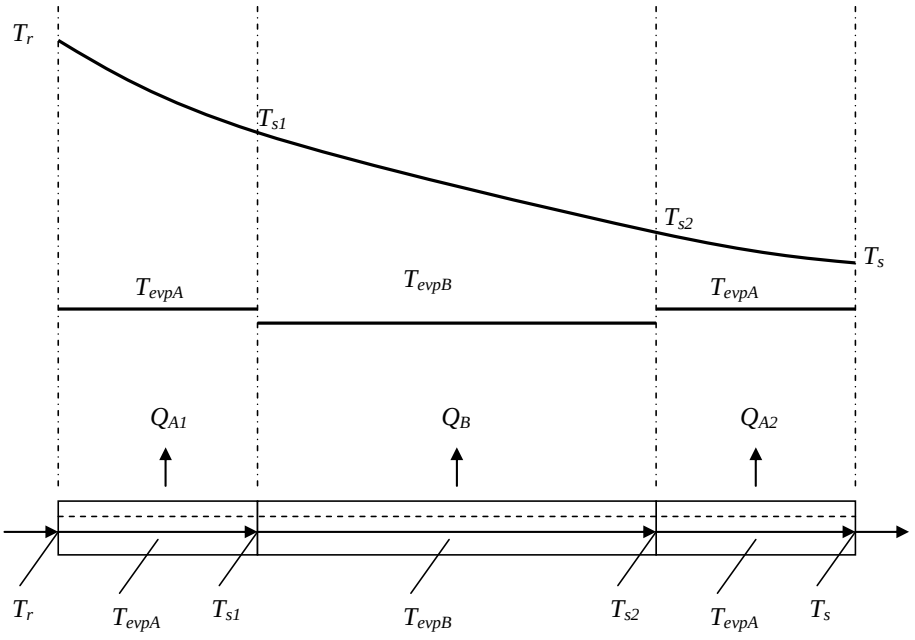

Figure 6 The three-heat-exchanger model for the evaporator

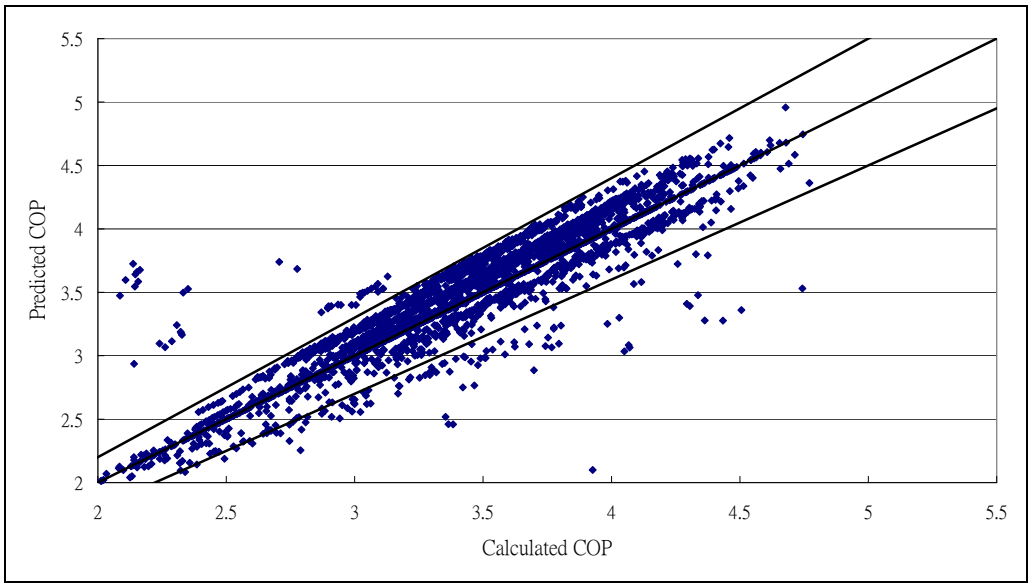

Figure 7 Comparison of COP predicted by the model and calculated from plant operating data

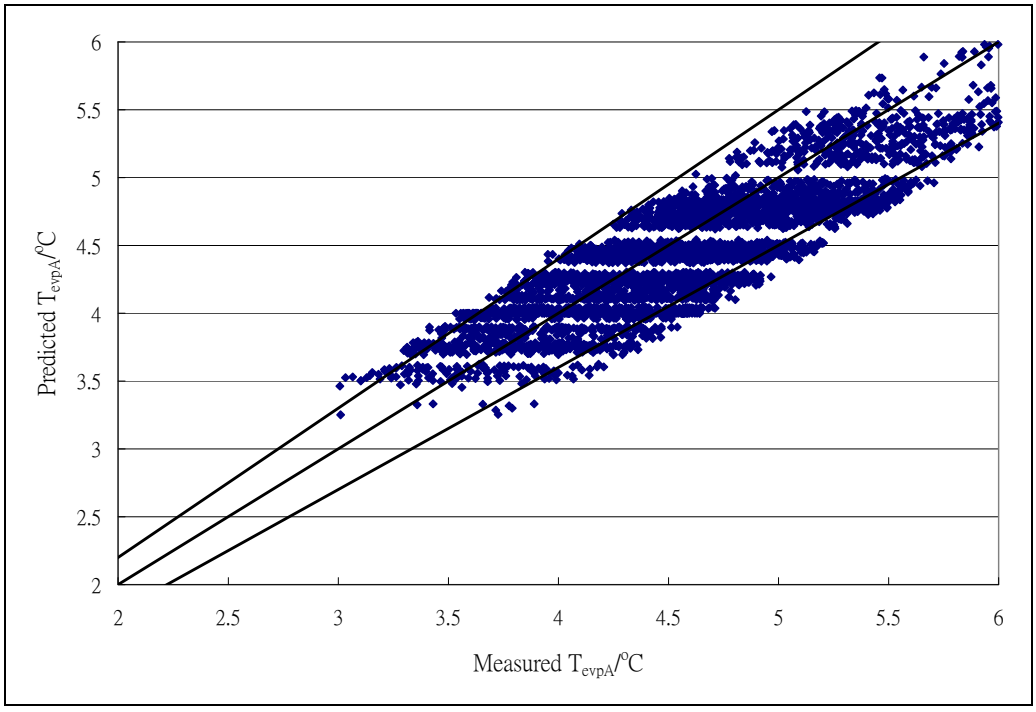

Figure 8 Comparison between predicted and measured evaporating temperature at circuit A

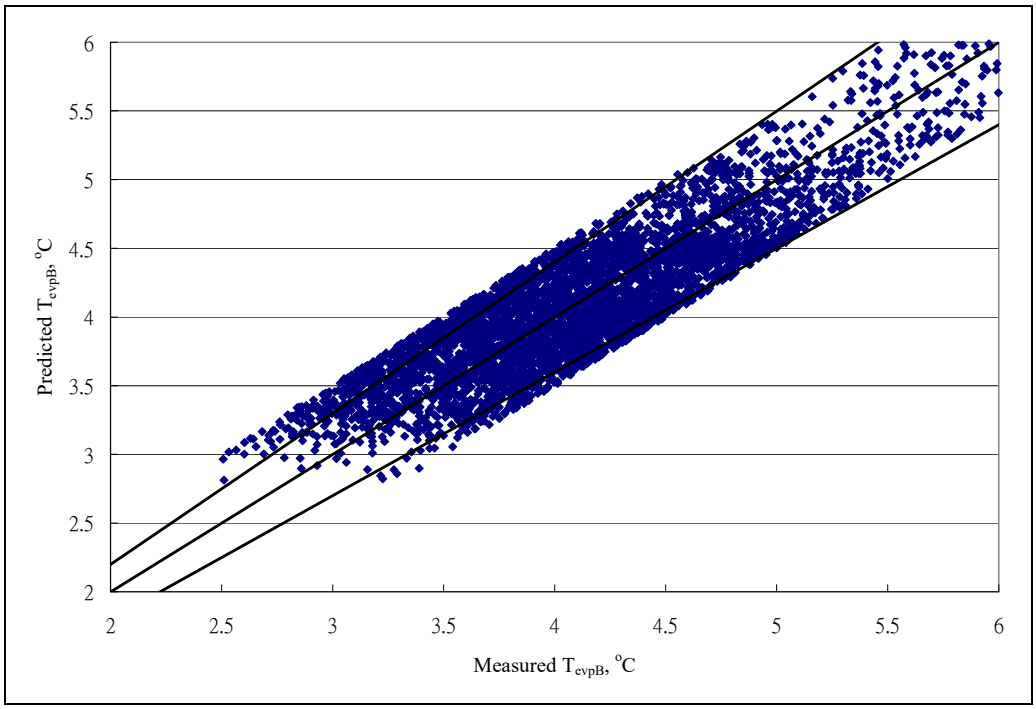

Figure 9 Comparison between predicted and measured evaporating temperature at circuit B

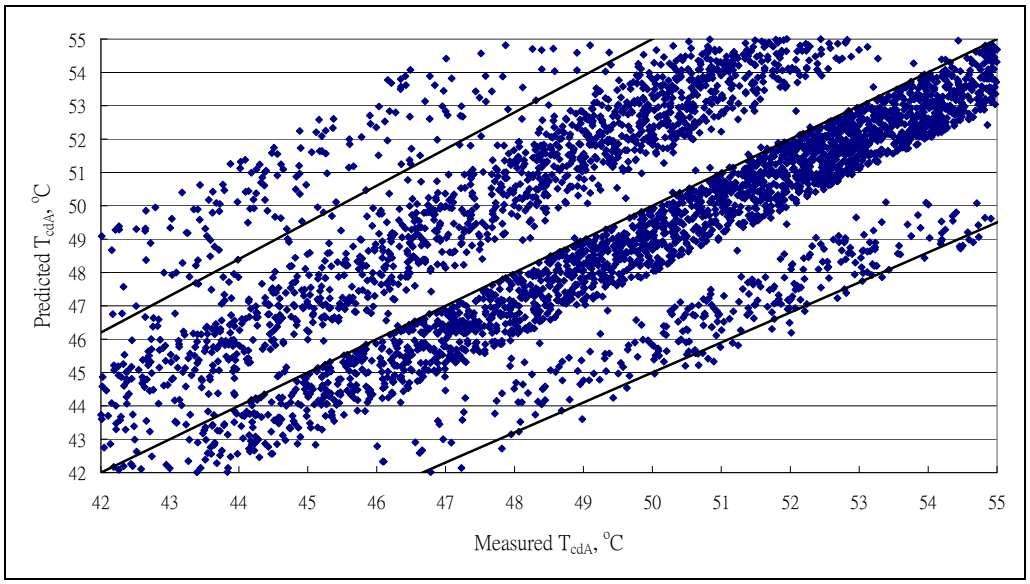

Figure 10 Comparison between predicted and measured condensing temperature at circuit A

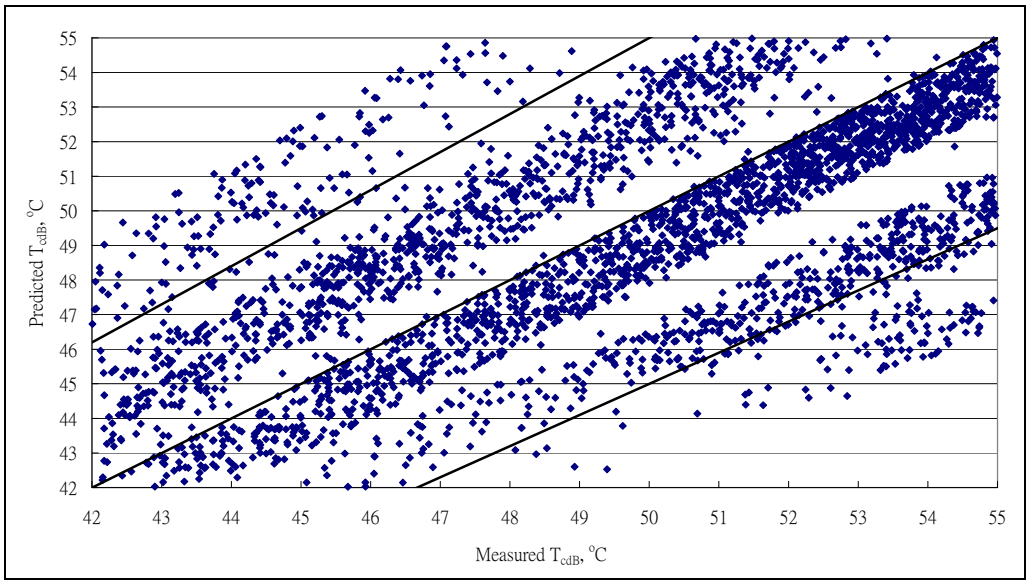

Figure 11 Comparison between predicted and measured condensing temperature at circuit B

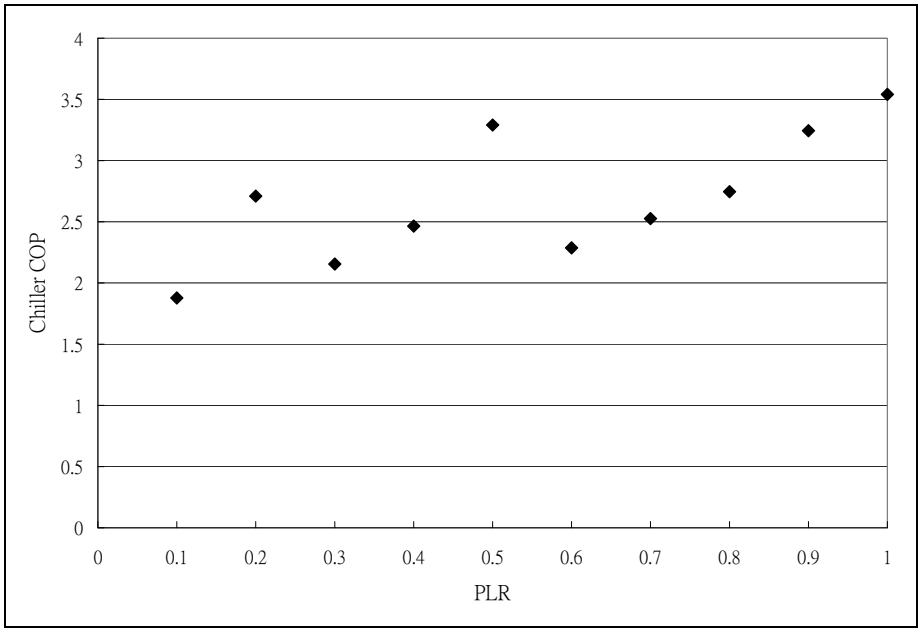

Figure 12 Change in chiller *COP* with *PLR*: Model predictions

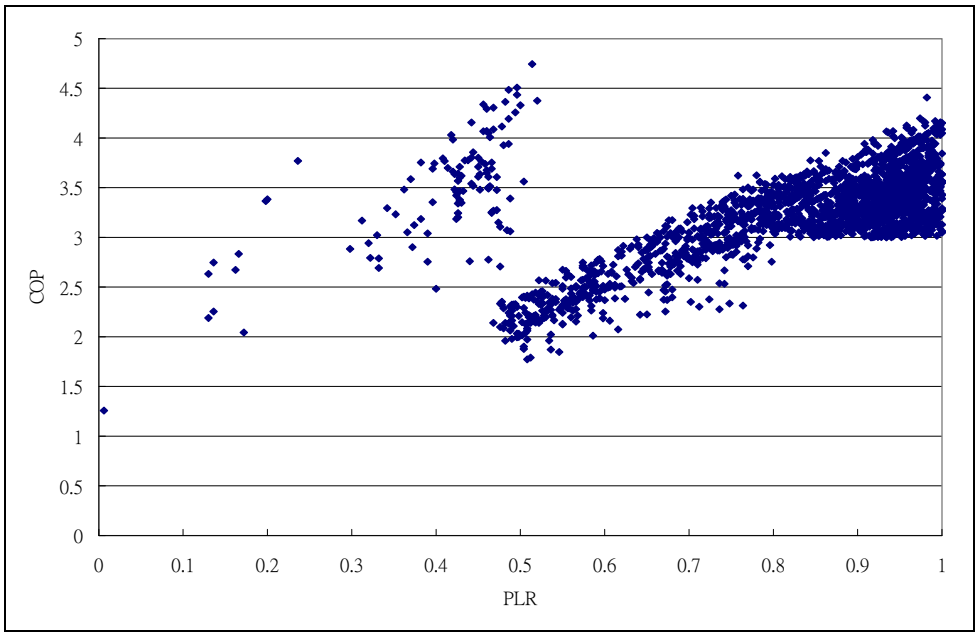

Figure 13 Change in chiller *COP* with *PLR*: Measured data